

## Crystallization Kinetics of Poly(phenylene sulfide) Containing a Thermotropic Liquid Crystalline Polyesteramide

Soon Man HONG,<sup>†</sup> Byoung Chul KIM, Kwang Ung KIM,  
and In Jae CHUNG\*

*Polymer Processing Laboratory,  
Korea Institute of Science and Technology,  
P.O. Box 131, Cheongryang, Seoul, Korea 130-650  
\*Department of Chemical Engineering,  
Korea Advanced Institute of Science and Technology,  
373-1 Kusong-dong, Yusong-gu, Taejeon, Korea 305-701*

(Received July 29, 1991)

**ABSTRACT:** Isothermal and nonisothermal crystallization kinetics of poly(phenylene sulfide) (PPS) including a thermotropic liquid crystalline polyesteramide (LCP) have been investigated by means of Avrami and Ozawa expressions. As the LCP content is increased, the supercooling required for PPS crystallization, both half time for crystallization and size of spherulites decrease. Further, the PPS containing LCP exhibits a higher nucleation density than pure PPS when three dimensional growth and constant radial growth rate of spherulites are assumed. In the nonisothermal crystallization process, PPS/LCP blend systems exhibit a notable reduction in Avrami exponent. In the isothermal process, the radius of spherulite linearly increases with time.

**KEY WORDS** Poly(phenylene sulfide) / Liquid Crystalline Polyesteramide / Blend / Nucleation / Crystallization / Avrami-Ozawa /

Poly(phenylene sulfide) (PPS) is a linear polymer with dual properties of thermoplastic and thermoset. That is, heating this thermoplastic in air substantially increases its melt viscosity.<sup>1</sup> The mechanical properties of crystalline PPS are highly dependent on the processing conditions which govern the crystallization process. Much effort has been made to describe the crystallization kinetics and morphology of PPS.<sup>1-11</sup> In general, crystallization proceeds *via* homogeneous and/or heterogeneous nucleation, followed by growth of the nucleated spherulites. Nucleating agents include inorganic additives such as talc, chalk, glass and silica, organic compounds such as salts of mono or polycarboxylic acids, and polymers such as high density polyethylene

(HDPE) and liquid crystalline polyesteramide (LCP).<sup>3,4,12</sup> It has been fairly well recognized that the presence of a nucleating polymer has a profound influence on the crystallization kinetics of crystalline PPS.<sup>2-4</sup> The higher crystallization rate by incorporating a nucleating polymer improves productivity by shortening the molding cycle.<sup>3</sup> Further, it leads to heterogeneous nucleation and consequently enhances the properties of the molded parts by developing finer grain structure.<sup>1,10,11</sup>

In the present paper, we investigate the effects of a thermotropic liquid crystalline copolyesteramide on the isothermal and nonisothermal crystallization kinetics of PPS by analyzing DSC and polarized optical microscope data adopting Avrami and Ozawa equ-

\* To whom all correspondences should be addressed.

ations.

## EXPERIMENTAL

### *Sample Preparation*

PPS used was a commercial grade Ryton GR-02 manufactured by Phillips Petroleum Co. and thermotropic copolyesteramide (LCP) tested as nucleating agent was Vectra B950 manufactured by Hoechst Celanese Co. The copolyesteramide was composed of 2,6-hydroxynaphthoic acid (60%), terephthalic acid (20%), and aminophenol (20%). Both polymers were dried at 100°C in a forced convection oven at least 24 h prior to use. The content of LCP in the blends was 3, 5, 10, 25, 50, and 75 wt/wt%. The mixed compound was prepared by melt extruding the formulated components in a Brabender twin-screw extruder, quenching in a water bath, followed by drawing and pelletizing. The temperature of barrel and die was controlled at 290°C for PPS, at 300°C for LCP, and at intermediate of two temperatures for PPS/LCP blend systems depending on the composition.

### *Measurements of Crystallization Kinetics*

Thermal properties were measured with a Du Pont 2000 thermal analyzer equipped with a 910 DSC apparatus. The heat of fusion and heat of crystallization were determined from the peak area on the DSC curve. Isothermal crystallization data were obtained as follows. The sample was heated up to 330°C in a nitrogen atmosphere, and held at 330°C for 3 min. It was quenched at a rate of 160°C min<sup>-1</sup> to a predetermined crystallization temperature at which the exothermic crystallization peak was recorded. The total crystallization time was determined as the time required from the onset of the exothermic DSC traces at constant temperature until a steady baseline was obtained. The isothermal crystallization time was measured over the temperature range from 230 to 255°C for PPS. Nonisothermal crystallization experiments were carried out at several

cooling rates, 2, 4, 8, and 12°C min<sup>-1</sup>. The optical texture of PPS/LCP blends was observed by a Leitz Ortholux II microscope equipped with a heating stage and a programmable PID temperature controller model 350. To get the true temperature during the heating stage, calibrations were made for various crystalline materials with known melting points; maleic anhydride (mp = 52°C), naphthalene (80°C), benzoic acid (121°C), hydroquinone (171°C), hydroxy benzoic acid (213°C), anthraquinone (284.5°C), and sodium nitrate (306°C).<sup>10</sup> The radial growth rate of PPS spherulites and resultant morphology were also observed by the same microscope.

## RESULTS AND DISCUSSION

### *Thermal Behavior*

DSC curves of PPS/LCP blends are shown in Figure 1. Pure PPS exhibited a melting endotherm peak at 279°C and a glass transition temperature ( $T_g$ ) at 90°C. PPS rapidly crystallized above  $T_g$  as indicated by a cold exotherm crystallization peak ( $T_{cc}$ ) at 119°C. Similar results have been reported for quenched PPS samples by others.<sup>6-8</sup> It is seen that such thermal transitions as  $T_g$ ,  $T_m$ , and  $T_{cc}$  remain nearly unchanged with LCP content. This suggests that PPS and the copolyesteramide used in this work are almost incompatible in all compositions examined. The area under the crystallization and melting transition of PPS/LCP blends decrease with increasing LCP content. This seems to result from a small thermal effect of LCP, as shown in DSC curves of LCP rich phase.<sup>34</sup> In our case, the heat of cold crystallization ( $\Delta H_{cc}$ ) and heat of fusion ( $\Delta H_f$ ), normalized per gram of PPS homopolymer, did not show any clear tendency. However, it has been reported that heterogeneous nucleation decreases the crystallinity of PPS.<sup>2,5</sup> On the other hand, Sukhadia *et al.* suggest increase of crystallinity by the nucleation action of LCP.<sup>35</sup>

The melt crystallization exotherms of PPS

### Crystallization of PPS Containing LCP

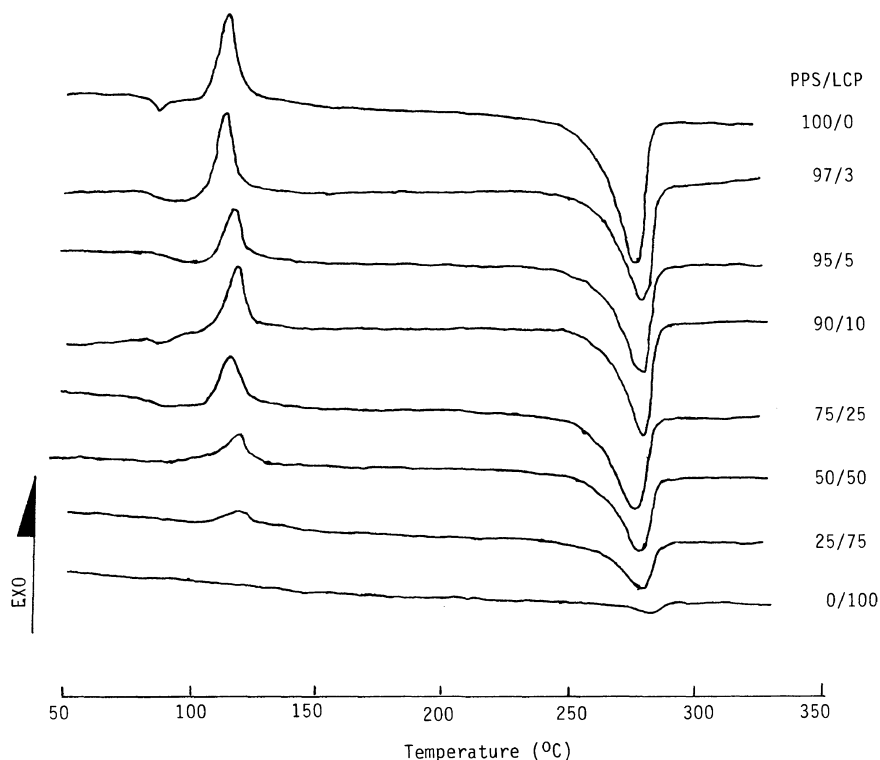


Figure 1. DSC thermograms of PPS/LCP blends at the heating rate  $10^{\circ}\text{C min}^{-1}$ .

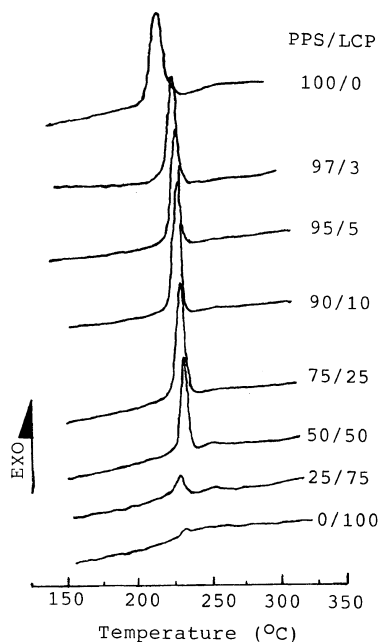


Figure 2. Crystallization exotherms of PPS/LCP blends at the cooling rate  $10^{\circ}\text{C min}^{-1}$ .

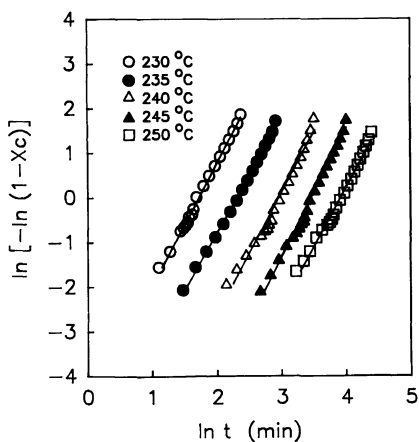
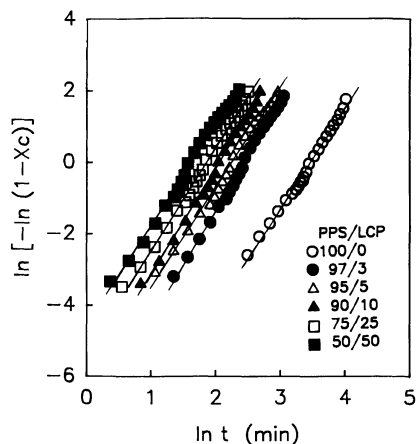
and PPS/LCP blend systems observed during the cooling stage are shown in Figure 2. The melt crystallization temperature ( $T_{mc}$ ) of PPS increased with LCP content up to 50 wt% because the LCP phases dispersed finely within the PPS matrix promotes heterogeneous nucleation.<sup>2-4,12</sup> On the other hand, LCP reduces the crystallization rate when LCP content was higher than 50 wt% probably due to the phase inversion.<sup>18-20</sup> The gradual decrease in apparent supercooling ( $\Delta T = T_p - T_o$ ;  $T_p$  is the melting peak temperature and  $T_o$  is the onset temperature of crystallization) further supports the validity of this explanation. The apparent supercooling required for initiating crystallization was  $57^{\circ}\text{C}$  for pure PPS. But it decreased to  $41^{\circ}\text{C}$  with increasing LCP content as shown in Table I.<sup>3,21</sup>

#### *Isothermal Crystallization Kinetics*

The Avrami equation which describes iso-

**Table I.** Thermal properties of several PPS/LCP blends

LCP	$T_g$	$T_{cc}$	$\Delta H_{cc}$	$T_m^a$	$\Delta H_f$	$T_{mc}^a$	$T_{mc}^b$	$\Delta H_{mc}$	$\Delta T^c$
%	°C	°C	J gm <sup>-1</sup> PPS	°C	J gm <sup>-1</sup> PPS	°C	°C	J	°C
0	90	119	11.7	279	34.9	206	222	35.3	57
3	89	119	12.1	280	31.1	221	233	32.1	47
5	88	119	10.1	280	30.6	222	234	30.4	46
10	87	120	10.5	280	32.2	224	232	35	48
25	85	119	16.9	280	36.7	226	238	38.5	42
50	86	119	17.5	279	38.2	229	238	38.3	41
75		120	7.1	279	41.2	226	236	27.6	43
100				282	( 1.4)	231	235	(0.67)	47

<sup>a</sup> Peak temperature.<sup>b</sup> Onset temperature on the cooling scan.<sup>c</sup>  $\Delta T$ , degree of supercooling.**Figure 3.** Avrami plots of isothermal crystallization of PPS at various temperatures.**Figure 4.** Avrami plots of isothermal crystallization of PPS/LCP blends at 245°C at various LCP contents.

thermal crystallization kinetics is defined by eq 1<sup>13</sup>;

$$X_c(t) = 1 - e^{-Kt} \quad (1)$$

where  $X_c(t)$  denotes the weight fraction of crystals at time  $t$  and at a constant temperature  $T$ ,  $K$ , a rate constant that includes the combined effects of nucleation and crystal growth rate, and  $n$ , the Avrami exponent depending on the dimension of crystal growth and the type of nucleation.<sup>14</sup> The Avrami exponent  $n$  can be determined from a plot of  $\ln[-\ln(1-X_c(t))]$  against  $\ln t$ .

The Avrami plots of PPS at several temperatures are shown in Figure 3, and those of PPS/LCP blend systems at 245°C are shown in Figure 4. It is clear that the Avrami equation fairly well describes the isothermal crystallization behavior of PPS and PPS/LCP blend systems. By these plots, two crystallization kinetic parameters,  $n$  and  $K$ , are determined using the least square method. The Avrami parameters derived from exothermic heat flow during melt crystallization are in agreement with the results obtained by Lopez and Wilkes<sup>10</sup> on the basis of the effect of molecular

weight of PPS. It should be noted that the values of the Avrami exponent  $n$  exhibited a narrow spread over the wide range of temperatures, and had a value of about 3. This indicates that spherulites are formed three dimensionally. This confirms that the assumption in eq 3,  $n=3$ , is almost valid for calculation of the nucleation densities. It further indicates the spherical growth of the crystalline structure on constant nucleation or the plate-like spherulites on sporadic nucleation.<sup>22</sup> The presence of LCP did not have any significant effect on the Avrami exponent.<sup>12</sup> This means that the nucleation mechanism and crystal growth geometries are similar for all samples.<sup>23</sup>

The rate constant  $K$  can be calculated by eq 2<sup>10,12</sup>;

$$K = \frac{\ln 2}{(t_{1/2})^n} \quad (2)$$

where the half-time of crystallization,  $t_{1/2}$ , is defined as the time at which the extent of crystallization is 50% complete.

The half-time of crystallization,  $t_{1/2}$ , is plotted against the isothermal crystallization temperature in Figure 5. Like other semi-crystalline polymers, the half-time of crystallization increased with isothermal crystallization

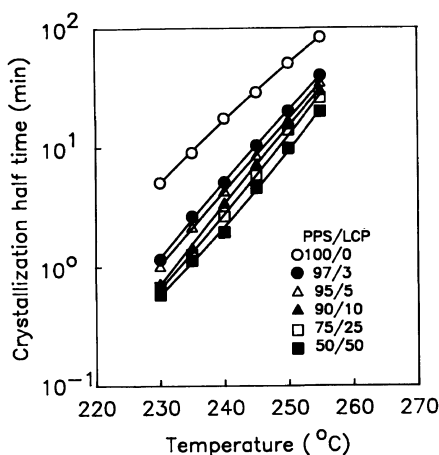


Figure 5. Variation of crystallization half-time for PPS/LCP blends with isothermal crystallization temperature.

temperature for all systems examined. The LCP component dramatically decreased the half-time of crystallization, particularly at lower crystallization temperatures. This accelerating effect of LCP is related to heterogeneous nucleation. Nadkarni *et al.*<sup>3-5</sup> reported that the crystallization of PPS was accelerated by glass due to the heterogeneous nucleation.

When we assume that nucleation results in three dimensional spherulites, and that the radial growth rate of spherulites is constant, the nucleation density  $N$  (number of nuclei/cm<sup>3</sup>) can be estimated by eq 3<sup>10</sup>;

$$N = \frac{3K}{4\pi G^3} \quad (3)$$

where  $G$  is the radial growth rate of crystals. Hence, the combination of  $K$  obtained from DSC experiments and  $G$  obtained by polarized optical microscopy on spherulite growth rates enables one to estimate the nucleation density as a function of crystallization temperature. The values of  $K$  might be corrected if the true values of the exponent  $n$  are known. We assume that the nucleation is purely instantaneous (*viz.*,  $n=3$ ) and thus the corrected value of the rate constant,  $K'$ , is given by eq 4<sup>15</sup>

$$K' = \frac{4}{3} NG^3 \cong (K_{\text{exp}})^{3/n} \quad (4)$$

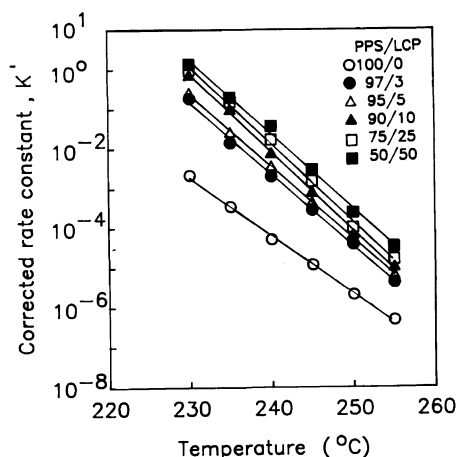


Figure 6. Corrected rate constants for PPS/LCP blends vs. isothermal crystallization temperature.

where  $K_{\text{exp}}$  denotes the rate constant obtained experimentally.

The rate constant,  $K$ , in eq 2 is corrected by eq 4, and plotted against the crystallization temperature in Figure 6. The overall rate constant decreased with increasing temperature, but increased as LCP content increased up to 50 wt%, as also reported by Lopez and Wilkes.<sup>10</sup>

The radial growth rate,  $G$ , of spherulites can be described by eq 5<sup>16,17</sup>;

$$\ln G = \ln G_0 - \left( \frac{\Delta E}{KT} + \frac{\Delta F^*}{KT} \right) \quad (5)$$

where  $\Delta E$  denotes the free energy of activation for a chain crossing the barrier to the crystal,  $\Delta F^*$ , the free energy of a surface nucleus of critical size, and  $k$ , the Boltzmann constant.

The radius of the spherulites originating from a single nucleus was measured as a function of isothermal crystallization temperatures by means of polarized optical micrograph.<sup>24,25</sup> The radial growth rate ( $G$ ) at a given isothermal crystallization temperature was also estimated by plotting the size of nucleus against time. The radial growth rate of a PPS spherulite so obtained is plotted against the reciprocal temperature in Figure 7. Referring to eq 5,  $\ln G_0$  and  $(\Delta E + \Delta F^*)/k$  can

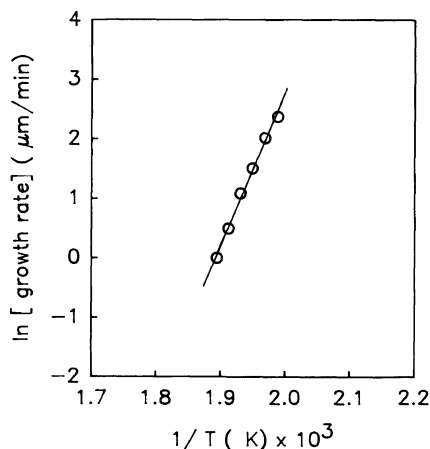


**Figure 7.** Relationship between  $\ln$ [growth rate of PPS] and  $1/T$ .

be determined from the intercept and slope of this linear plot, respectively. Utilizing the least square method, the radial growth rate of PPS spherulites with crystallization temperature can be empirically expressed by eq 6;

$$\ln G \text{ (}\mu\text{m min}^{-1}\text{)} = -48.4 + 25.58 \times \left[ \frac{1}{T \text{ (K)}} \times 10^3 \right] \quad (6)$$

This equation enables one to estimate the isothermal radial growth rate of PPS spherulites at a given crystallization temperature.

By applying the radial growth rate ( $G$ ) and corrected rate constant ( $K'$ ) to eq 3, the nucleation densities of pure and nucleated PPS were calculated and plotted against temperatures in Figure 8. It is seen that the nucleation density of PPS decreased as crystallization temperature increased. Further, with increasing temperature, the nucleation density diminished and larger spherulites resulted. Similar results have been reported by others.<sup>26,27</sup> On the whole, the nucleating density increased with LCP content. This implies that LCP phase produces more nucleating sites for the crystallization of PPS.

Figure 9 shows polarized optical micrographs of PPS and PPS/LCP blend systems at

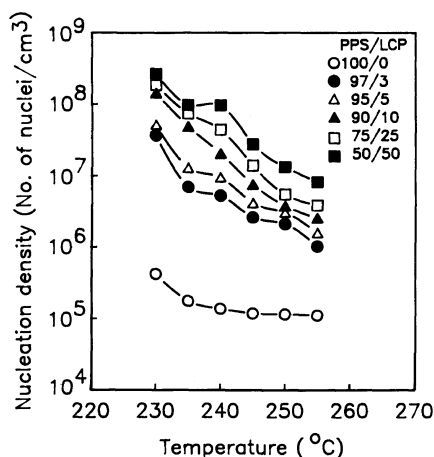


**Figure 8.** Number of effective nuclei vs. crystallization temperature for the PPS/LCP blends.

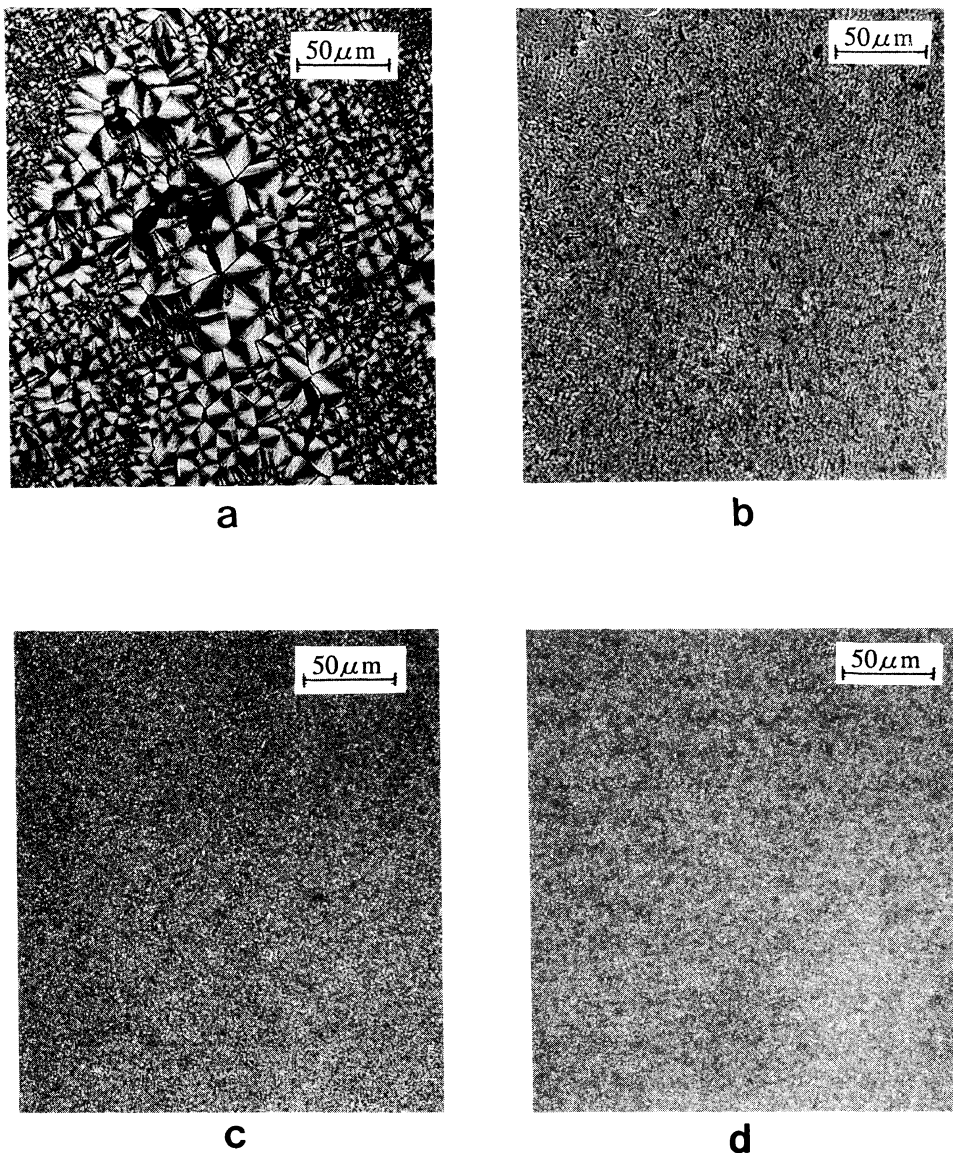


**Figure 9.** Polarized optical micrographs of PPS/LCP blends at the cooling rate  $8^{\circ}\text{C min}^{-1}$ . a, 100/0; b, 97/3; c, 95/5; d, 90/10.

a cooling rate  $8^{\circ}\text{C min}^{-1}$ . With nucleated PPS, grain spherulitic structures could be observed. On the other hand, pure PPS produced larger spherulites.

#### *Nonisothermal Crystallization Kinetics*

Most polymers are processed under non-isothermal conditions. It is therefore obvious

predicting crystallization kinetics under continuous cooling conditions is of primary practical importance. In addition, isothermal measurements are often restricted to narrow temperature ranges because the response time of the measuring instrument becomes comparable to the overall time for crystallization. Consequently, nonisothermal experiments during

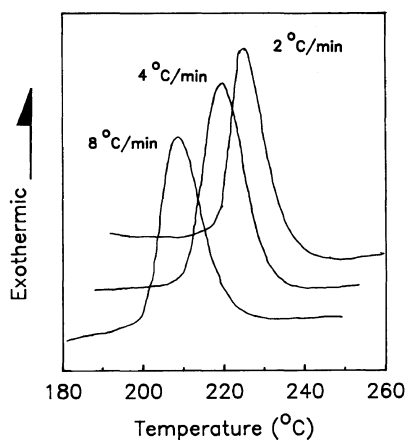


**Figure 10.** Typical DSC thermograms of the non-isothermal crystallization of PPS.

cooling can offer a clue to understand the crystallization behavior of polymers.<sup>11,28–30</sup> Nonisothermal crystallization kinetics can be obtained by applying the nonisothermal DSC data to the Ozawa equation, an extended Avrami equation.<sup>28</sup> Ozawa assumes that crystallization occurs at a constant cooling rate, and that crystallization originates from a distribution of nuclei that grow as spherulites with constant radial growth rate at a given temperature. The weight fraction of the crystallized material at time  $t$  is defined by eq 7;

$$\ln\{\ln(1 - X_c(t))\} = \chi - n \ln \phi \quad (7)$$

where  $n$  represents the Avrami exponent,  $\chi$ , cooling crystallization function, and,  $\phi$ , cooling rate.

Typical DSC curves of neat PPS obtained in the nonisothermal crystallization process are shown in Figure 10. At each cooling rate, crystallization took place at temperatures above the peak temperature of crystallization, suggesting that transformation is controlled by nucleation. Nucleation occurs at higher temperatures when the polymer sample is cooled at slower scanning rates because there is a sufficient time to activate nuclei at higher temperatures. The activation of nuclei occurs at lower temperatures at faster cooling rates.

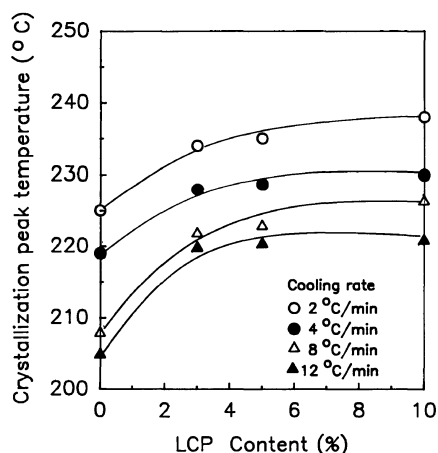


**Figure 11.** Variation of crystallization peak temperature of PPS/LCP blends with the cooling rate.

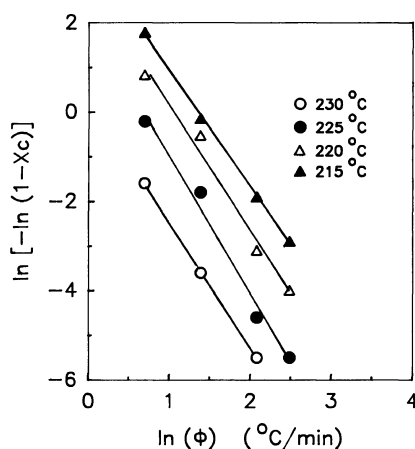


**Figure 12.** Ozawa plot of non-isothermal crystallization for neat PPS.

Changes in the crystallization peak temperatures of neat and nucleated PPS as a function of the LCP content at different cooling rates are shown in Figure 11. At a fixed LCP level, the crystallization peak temperature decreased with increasing cooling rate. At a given cooling rate, however, the crystallization peak temperature increased as LCP content increased.

Ozawa plots of PPS and PPS/LCP blend systems by adopting eq 7 are shown in Figures 12 and 13, respectively. Linearity at a given temperature shows the experimental data to



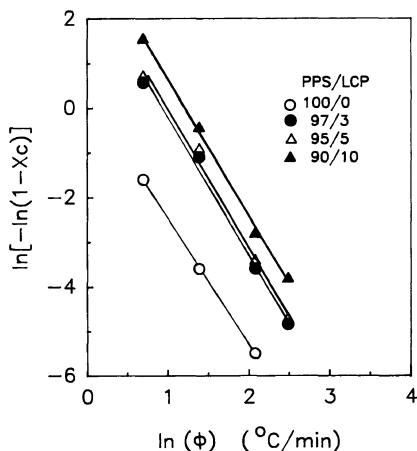


Figure 13. Ozawa plot of non-isothermal crystallization for PPS/LCP blends.

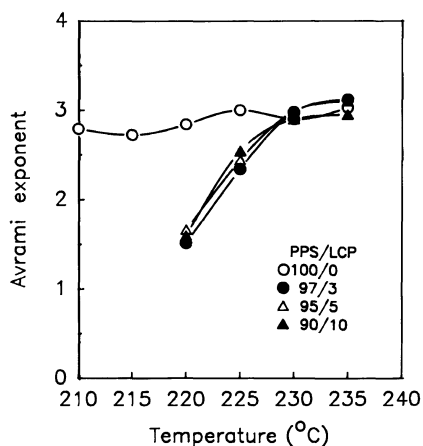


Figure 14. Plot of Avrami exponent vs. temperature for PPS/LCP blends.

be consistent with the theory of Ozawa's.<sup>28</sup> Further, the absence of curvature in polyethylene and poly(ether-ether-ke-ton) rules out the possibility of secondary crystallization.<sup>29,31</sup>

The Avrami exponent  $n$  can also be determined from Ozawa plots, and the slope on the plot of  $\ln[-\ln(1-X_c)]$  against  $\ln(\phi)$  by the least square method. In determination of the exponent, the crystalline weight fraction should be less than 0.5 because the effect of impingement, truncation of spherulites, and secondary crystallization kinetics might become very important at higher crystalline fractions.<sup>11,29</sup> The Avrami exponents so obtained are plotted against temperature in Figure 14. Pure PPS gives a value of about three, suggesting that the nucleated process leads to a spherulitic growth with thermal nucleation.<sup>23,25,26</sup> In case of PPS/LCP blend systems, however, the Avrami exponent decreases as temperature decreases, particularly at low crystallization temperatures. This implies that the nucleated process leads to rod-shaped growth with thermal nucleation.<sup>23,25</sup> Two factors that lower the value of  $n$  are worth mentioning. First, a fast crystallization rate of the blend systems at lower temperatures prevents the spherulite from developing into 3 dimensional crystal-

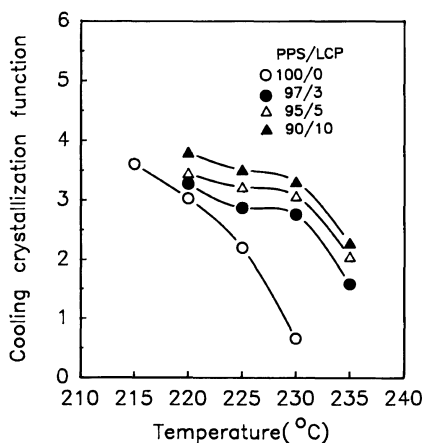


Figure 15. Plot of cooling crystallization function vs. temperature for PPS/LCP blends.

lites.<sup>11</sup> Secondly, growth site impingement, truncation of spherulites, impurity segregation, and slightly slow secondary crystallization may change the crystallization mechanism if the crystalline weight fraction is higher than 0.5.<sup>11,29,31-33</sup> However, at higher crystallization temperatures, *e.g.*, 230–235°C, the Avrami exponent becomes roughly equal to 3 because the predetermined nuclei grow into 3 dimensional spherulites before cooled.<sup>22,29</sup>

The intercept of the Ozawa plots give the cooling crystallization function which re-

presents the rate of nonisothermal crystallization.<sup>11,28,30</sup> The cooling crystallization function against temperature is presented in Figure 15. The function was increased with decreasing temperature or increase in LCP content. Similar results were reported by Ozawa<sup>28</sup> for PET, Kozłowski<sup>30</sup> for nylon, Elder *et al.*<sup>29</sup> for PP and Lopez *et al.*<sup>11</sup> for PPS.

## CONCLUSIONS

This paper provides evidence that LCP is a nucleating agent in both isothermal and nonisothermal crystallization of PPS. Experimental results of DSC and optical microscopy indicated the nucleation and crystal growth to be affected by the content of LCP as well as crystallization temperature. As the content of LCP increases, crystallization half time, size of spherulite, and extent of supercooling decrease. The number of nuclei in PPS increases as the content of LCP was increases and increases exponentially as the crystallization temperature decreases.

## REFERENCES

1. C. C. M. Ma and L. T. Hsiue, *J. Appl. Polym. Sci.*, **39**, 1399 (1990).
2. G. P. Desio and L. Rebenfeld, *J. Appl. Polym. Sci.*, **39**, 825 (1990).
3. V. M. Nadkarni and J. P. Jog, *J. Appl. Polym. Sci.*, **32**, 5817 (1986).
4. V. M. Nadkarni, V. L. Shingankuli, and J. P. Jog, *Intern. Polym. Proc.*, **2**(1), 55 (1987).
5. J. P. Jog and V. M. Nadkarni, *J. Appl. Polym. Sci.*, **30**, 997 (1985).
6. D. G. Brady, *J. Applm. Poly. Sci.*, **20**, 2541 (1976).
7. S. S. Song, J. L. White, and M. Cakmak, *Intern. Polym. Proc.*, **4**(2), 96 (1989).
8. E. Maemura, M. Cakmak, and J. L. White, *Intern. Polym. Proc.*, **3**(2), 79 (1988).
9. H. W. Hill and D. G. Brady, *Polym. Eng. Sci.*, **16**(12), 831 (1976).
10. L. C. Lopez and G. L. Wilkes, *Polymer*, **29**, 106 (1988).
11. L. C. Lopez and G. L. Wilkes, *Polymer*, **30**, 882 (1989).
12. S. H. Jung, Ph.D. Dissertation, Korea Advanced Institute of Science and Technology (KAIST), 1988.
13. L. Mandelkern, "Crystallization of Polymers," McGraw-Hill, New York, N.Y., 1964.
14. C. N. Velisaris and J. C. Seferis, *Polym. Eng. Sci.*, **26**(22), 1574 (1986).
15. T. Kowalewski and A. Galeski, *J. Appl. Polym. Sci.*, **32**, 2919 (1986).
16. J. I. Laurizen, Jr. and J. D. Hoffman, *J. Res. Natl. Bur. Stand (A)*, **64**, 73 (1960).
17. H. D. Keith and F. J. Padden, Jr., *J. Appl. Phys.*, **35**, 1270 (1964).
18. M. R. Nobile, E. Amendola, L. Nicolais, D. Acierno, and C. Carfagna, *Polym. Eng. Sci.*, **29**, 224 (1989).
19. A. Kohli, N. Chung, and R. A. Weiss, *Polym. Eng. Sci.*, **29**(9), 573 (1989).
20. C. U. Ko and G. L. Wilkes, *J. Appl. Polym. Sci.*, **37**, 3063 (1989).
21. Y. Lee and R. S. Porteer, *Polym. Eng. Sci.*, **26**(9), 633 (1986).
22. S. A. Jabarin, *J. Appl. Polym. Sci.*, **34**, 85 (1987).
23. M. Day, T. Suprunchuk, J. D. Cooney, and D. M. Wiles, *J. Appl. Polym. Sci.*, **36**, 1097 (1988).
24. S. Chew, J. R. Griffiths, and Z. H. Stanchurski, *Polymer*, **30**, 874 (1989).
25. Y. Deslandes, M. Dat, N. F. Sabir, and T. Suprunchuk, *Polym. Composites*, **10**(5), 360 (1989).
26. S. Kumar, D. P. Anderson, and W. W. Adams, *Polymer*, **27**, 329 (1986).
27. F. Rybnikar, *J. Appl. Polym. Sci.*, **27**, 1479 (1982).
28. T. Ozawa, *Polymer*, **12**, 150 (1971).
29. M. Eder and A. Wlochowicz, *Polymer*, **24**, 1593 (1983).
30. W. Kozłowski, *J. Polym. Sci., C*, **38**, 47 (1970).
31. P. Cebe and S. D. Hong, *Polymer*, **27**, 1183 (1986).
32. M. C. Tobin, *J. Polym. Sci., Polym. Phys.*, **14**, 2253 (1976).
33. S. P. Kim and S. C. Kim, *Polym. Eng. Sci.*, **31**(2), 110 (1991).
34. F. P. L. Mantia, A. Valenza, M. Paci, and P. L. Magagnini, *Rheol. Acta*, **28**(5), 417 (1989).
35. A. M. Sukhadia, D. Done, and D. G. Baird, *Polym. Eng. Sci.*, **30**(9), 519 (1990).